R. & M. No. 2716
(11,246)
A.R.C. Technical Report

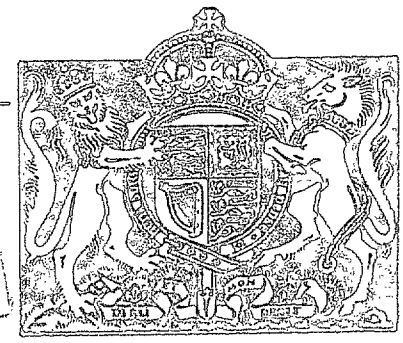

MINISTRY OF SUPPLY

AERONAUTICAL RESEARCH COUNCIL
REPORTS AND MEMORANDA

The Drag Increase at High Subsonic Speeds

By

K. OSWATITSCH

LONDON: HER MAJESTY'S STATIONERY OFFICE
1954
FIVE SHILLINGS NET

The Drag Increase at High Subsonic Speeds

By

K. OSWATITSCH*

COMMUNICATED BY THE PRINCIPAL DIRECTOR OF SCIENTIFIC RESEARCH (AIR), MINISTRY OF SUPPLY

Reports and Memoranda No. 2716†

October, 1947

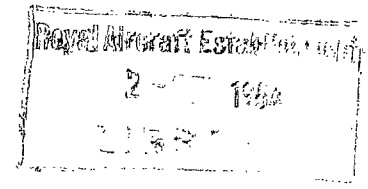

Summary.—The drag increase beyond the critical Mach number is calculated by modifying the supersonic part of the Kármán-Tsien pressure distribution on a profile. This is possible when the supersonic regions are not too large. The formula giving the modified pressure distribution is derived very roughly. It may give only one of the main effects appearing when supersonic speeds occur in the flow, and may be changed and calculated more exactly later.

For the calculation of the drag increase the formula is sufficient and the agreement of theory and experiment in all examples calculated is good. Within the approximation of the theory the lift coefficient is practically unchanged. Calculations of the centre of pressure are not made.

1. *Introduction.*—At Mach numbers little higher than the, so-called, critical Mach number, where at one point on the surface sonic speed is just reached, the drag coefficient of bodies increases very steeply to several times the low-speed value. As this increase of drag coefficient appears at very different distances from the critical Mach number depending on the body's shape, and limits the speed of many high-speed aircraft, it is very desirable to be able to estimate it.

Supersonic streams have the property that the flow is affected only in a certain region downstream of a point of disturbance. Hence the highest velocities, *i.e.*, the highest suction, appear further downstream than would be expected on high-subsonic theory. This move of suction to a more negative angle of profile inclination gives a drag increase. It depends not only on the change in the pressure distribution but also on the change of cross-section at the supersonic region. Thus in the case of a small supersonic region appearing near the maximum thickness the drag is very small.

The pressure distribution given by high-subsonic theory up and downstream of the supersonic region is quite good. In the absence of vorticity we can say that the supersonic velocity distribution has to be changed in such a manner that the area of the graph of velocity plotted against the length of the profile remains unchanged. This area condition leaves the lift coefficient practically unchanged within our approximations.

* The author having left the country before arrangements for publication were put in hand this report has been revised for publication at the Royal Aircraft Establishment.

† R.A.E. Tech. Note Aero. 1919, received 11th February, 1948.

Because of the steep pressure increase in the range of Mach numbers considered, a quite rough estimate of the change in the pressure distribution leads to a good theory for the drag increase. It agrees very well with tests in all the examples calculated.

2. *The Integral Equation for the Absence of Vorticity.*—To investigate the compressible flow round a body we take the integral equation of continuity :—

$$\iint_S \rho V_n \, d_S = 0 \; ; \qquad \ldots \ldots \ldots \ldots \ldots \ldots \ldots \ldots \qquad (1)$$

where S is a surface with the normal n, ρ the density and V the velocity. V_n is the velocity-component normal to the surface.

Further we take the integral form of the equation for absence of vorticity

$$\int_C V_t \, dl = 0 \qquad \ldots \ldots \ldots \ldots \ldots \ldots \ldots \ldots \qquad (2)$$

where C is a curve with the element of length dl and V_t (t = tangent) the component of velocity in the direction of the curve.

In this paper we disregard drag caused by friction, and separation, also induced drag. Hence drag can be caused only by the entropy increase in shock-waves[1]. It might seem that absence of vorticity is then not applicable ; but the drag depends on the product of shock height and shock loss, while the vorticity depends on the ratio of shock loss and shock height. Since the drag in transonic flow is always caused by relatively small losses in high shock-waves, we can neglect the influence of shock-waves on vorticity and use equation (2) for a first approximation, as shown also by Guderley[2].

The application of equation (1) on the surface of the body gives no interesting results.

To apply equation (2) we consider a streamline beginning far upstream of a body in an infinite flow, reaching the forward stagnation point, going from there in the direction of the flow along the body to the trailing stagnation point and then far downstream. This streamline we complete to a closed curve by two straight lines perpendicular to the stream and one straight line parallel to the stream at a great distance from the body. The application of equation (2) to this closed curve in subsonic flow gives

$$\int_{\text{streamline}} (V_t - V_\infty) dl = 0 \; ; \qquad \ldots \ldots \ldots \ldots \ldots \ldots \ldots \qquad (2a)$$

(V_∞ = velocity in the undisturbed flow), *i.e.*, the integral of the supervelocity along a streamline is equal to zero. Thus the area formed by the subvelocity plotted over the length of the streamline near the stagnation points (Fig. 1) is equal to the corresponding area formed by the supervelocities near the maximum thickness.

It can be shown that for two-dimensional supersonic flow also, equation (2a) is valid within a first approximation, *i.e.*, with linearisation of the compressible flow equation. The area of subvelocities ahead of the maximum thickness is equal to the area of supervelocities downstream of the maximum thickness.

In the second approximation for supersonic flow the two areas mentioned are different, for it is not possible to apply equation (2a) on a curve similar to the curve used for subsonic flow. Downstream of the body there are in supersonic flow subvelocities of the third order caused by entropy increases in the shock-waves. Integrating these subvelocities over a very long range of the x-axis, we get an error of the second order, *i.e.*, in general we get errors of the second order, if we apply equation (2) on very long curves. This remark is made for completeness, and is not of consequence in the following rough suggestions.

At subsonic speed (Fig. 1) there are pressures and suctions before and behind the maximum thickness. The pressure distribution is of such a kind that the drag is zero according to the

paradox of d'Alembert. At supersonic speed (Fig. 2) the pressures upstream and the suctions downstream of the maximum thickness give a drag. From the energy viewpoint this drag is caused by the heating of the air due to the shock-wave losses. At transonic speeds in the range of steeply increasing drag we have to assume shock-waves in the local supersonic field, otherwise drag cannot appear[1]. As we disregard separation, shock-waves on the surface have to be normal.

At subsonic speed with local supersonic regions disturbances disappear at great distance from the body as with pure subsonic speed. The effect of the local supersonic field corresponds to a greater volume of the body. Thus equation (2a) is valid also at transonic speed. In this range of speeds we must expect a velocity distribution similar to Fig. 1 with deviations chiefly near the highest velocities, but with equal areas formed by sub- and supervelocities.

3. *The Influence of Disturbances in Subsonic Flow.*—To investigate the influence of a small disturbance in two-dimensional *incompressible* flow, we consider the velocity distribution caused by a doublet, *i.e.*, the flow round a circular cylinder. At great distance from any disturbance in two-dimensional flow the velocity distribution is of this kind. In fact a very slender aerofoil corresponds to a circular cylinder of smaller area. In the case of small disturbances or great distances the disturbance of the velocity is the same as that of the x-component

$$\Delta u = A \frac{y^2 - x^2}{r^4}; \qquad \ldots \ldots \ldots \ldots \ldots \ldots \ldots \qquad (3)$$

$r = (x^2 + y^2)^{1/2}$ is the distance from the doublet, A is constant. It is the area of the circular cross-section of the cylinder and must be very small compared with r^2.

According to equation (3), in the 45 deg direction from the small body, there is, in two-dimensional flow, no disturbance of the velocity (Fig. 3). In front of the body, and downstream, there are subvelocities due to the stagnation effect. Laterally to the body there are supervelocities due to the acceleration of the flow caused by smaller separation of the streamlines. In any given direction the disturbance decreases in inverse proportion to the square of the distance.

According to the Prandtl rule, in the case of small disturbances, we can obtain the velocity distribution in a compressible flow by taking the velocity distribution of incompressible flow and multiplying u and y by the Prandtl factor

$$\beta = (1 - M_\infty{}^2)^{1/2}$$

(M_∞ = Mach number in the undisturbed flow).

Thus equation (3) becomes

$$\Delta u = \frac{A}{\beta} \frac{\beta^2 y^2 - x^2}{(\beta^2 y^2 + x^2)^2} \qquad \ldots \ldots \ldots \ldots \ldots \ldots \ldots \qquad (4)$$

The disturbance vanishes on the straight lines (Fig. 4)

$$\beta y = \pm x. \qquad \ldots \ldots \ldots \ldots \ldots \ldots \ldots \qquad (5)$$

The supervelocities appear now in a smaller range of angles. On the other hand the effect of the body across the mean flow exceeds the effect in the direction of the mean flow by the factor $1/\beta^2$. In these two directions the disturbance falls off as in the incompressible flow, inversely as the square of the distance.

Figs. 3a and 4a show the curves of constant perturbation for the Mach numbers $M_\infty = 0$ and $M_\infty = 0{\cdot}80$. Putting the function for the inner curves equal to 1 and -1 we get the other curves given in Figs. 3a and 4a. We will use the curves in the following to consider the influence of disturbances in the flow at a certain point of a profile.

We see that in subsonic flow the influence of profile parts far from the point considered is very small. The velocity at a given part of the surface depends chiefly on the shape in its near neighbourhood and on the velocity in the undisturbed flow. Within the Prandtl approximation

the *fractional* change in supervelocity Δu is the same on changing the shape, as the induced velocity of the changed part is like all supervelocities proportional to $1/\beta$. Thus if the local region of supersonic speed is small, the prediction of subsonic velocity distributions is expected to be quite accurate and the more so for improvements on the Prandtl approximation.

Supersonic velocities usually increase in the direction of the flow along convex-shaped bodies. This property of pure supersonic flow we can observe also with local supersonic fields. Since the velocity decreases in the y-direction and the mass flow decreases with increasing supersonic speed there are never difficulties in getting all the airmass from upstream to flow along the body. In subsonic flow the appearance of supersonic velocities brings a loss in mass flow. So the velocities with the highest mass flow—*i.e.*, the velocities near the speed of sound—have to cover a large part of the y-axis. This is only possible if the curvature of the streamlines, which is responsible for the velocity gradient in the y-direction, decreases quickly enough and this favours an increase of velocity along the surface. Thus it is not surprising that local supersonic fields in general have an asymmetric character, with higher velocities downstream.

The Prandtl rule corresponds to an approximation of the mass flow curve by a straight line (Fig. 5) and gives too high a mass flow in all parts of the flow except in the undisturbed state itself. Hence especially the supersonic velocities appearing in the subsonic flow have the effect of small doublets. According to equation (3a) the local supersonic field induces subvelocities far upstream and far downstream but the most important effect on the shape is in the supersonic region itself.

Considering a point on the profile just ahead of the sonic line (Fig. 6), we see that the local supersonic field lies in the stagnation region bounded by the two straight lines of equation (5). Hence the velocity at such a point is expected to be smaller than would be given by the Prandtl rule. It is very difficult to make any prediction about this error of the Prandtl rule in the supersonic region. Parts of the supersonic field induce sub- and supervelocities at a given point of the aerofoil. As we do not know the velocity distribution in the flow we cannot find the resultant effect. For a point just behind the supersonic region the induced velocities are in general expected to be smaller than for a point ahead of the region. According to Fig. 4a parts of the supersonic field induce here subvelocities, but other parts of equal influence induce supervelocities.

An iteration beginning with the velocity distribution given by the Prandtl rule—such as the iteration in the well-known Rayleigh-Jantzen method—does not succeed in the local supersonic region.

Comparing the Prandtl rule and improvements on it with tests, we find fairly good agreement downstream of the supersonic region (Figs. 9, 12, 15 and 16), if the latter is not too large. As expected the test velocities just ahead of the supersonic region are less than those given by high subsonic theory as the mass flow assumed in the Kármán-Tsien formula is also too high. Owing to the very steep increase of velocity on this part of the body, the error appears as a displacement of the sonic point a little downstream. Plotting the velocity along the x-axis, the error appears very small. Nevertheless, it can become important for the drag, because at this part of the profile the angle of flow is not small.

4. *The Distribution of Supersonic Velocities along the Profile.*—We assume we have a theoretical velocity distribution along the profile, which reproduces the subsonic part correctly and satisfies equation (2a). The drag calculated by this theoretical distribution, according to the principle of d'Alembert, is zero. The area given by the supersonic velocities plotted over the arc length is then the same as the corresponding area of the unknown (correct) supersonic velocity distribution.

But the highest velocities are expected to move downstream, owing to the property of supersonic flow of influencing points downstream only. Assuming a supersonic velocity increase ending with a normal shock-wave together with the area condition—equation (2a)—the supersonic velocity distribution should be quite determined. A normal shock-wave near sonic speed implies

that the speed of sound is just the mean of the velocities immediately before and behind the shock. In our theory of small supersonic fields, *i.e.*, of small supersonic velocities, this means that the pressure coefficient corresponding to sonic speed is the mean of the pressure coefficients just before and behind the shock. This result is contrary to nearly all test results. Thus theoretically we should assume at first a continuous compression in the supersonic region ending with a normal shock-wave, or no shock-wave on the wall at all. Owing to boundary-layer properties[3] such a continuous compression seems not to be possible without separation. Hence we have to assume λ-shocks in the tests as shown by Ackeret[4], and at higher local supersonic speed fork shocks or inclined shock-waves with only a short region of separation. The latter seem to be possible in the case of small supersonic speeds, where an inclined shock-wave causes a very small deflection of the flow only.

For estimating the downstream move in the supersonic region we can make the following suggestions. Owing to the rapid decrease of Mach angle α with increasing Mach number M (Table 1)

TABLE 1

M	1·000	1·084	1·133	1·22
α	90 deg	67 deg	62 deg	55 deg

the main effect of assuming speeds to be slightly supersonic, does not seem to be a wrong distribution of stream angle along the sonic line or a great change in the form of the sonic line caused by taking high subsonic theory instead of exact calculation ; it seems to come from the property of supersonics of influencing downstream only rather than chiefly across the flow as at high subsonic speed. So we can expect that all supersonic speeds appear a distance Δx more downstream than is given by high subsonic theory. This distance depends on the height h of the supersonic region at the point investigated and on the Mach angle there (Fig. 7). Taking an average Mach angle $\bar{\alpha}$ we find

$$\Delta x = h \cot \bar{\alpha} . \qquad (6)$$

The height h we estimate using the equation for absence of vorticity

$$\frac{1}{V}\frac{\partial V}{\partial y} = -\frac{1}{R}; \qquad (7)$$

R is the radius of curvature of the streamline. Assuming small stream angles we can take y for the direction perpendicular to the flow. The difference equation corresponding to equation (7) gives for the height h

$$h = \bar{R}\frac{V - V^*}{V_\infty} \qquad (7a)$$

where $\bar{R}$ is an average radius of curvature and V^* the critical velocity. The value of $\bar{R}$ we could approximate by the radius of curvature of the profile itself. Because of the large changes of $\bar{R}$ along the profile and since we want to know $\bar{R}$ in the neighbourhood of the highest supervelocities—and not on the point of maximum thickness—we estimate $\bar{R}$ at the highest supervelocity reached in the flow. As we shall always, in the following, use pressure coefficients c_p rather than velocities, and as we will calculate the compressible pressure distribution using the incompressible one, we estimate the average $\bar{R}$ from the highest pressure coefficient $c_{p0\,\max}$ obtained on a circular-arc of the radius $\bar{R}$ in incompressible flow. (c_p pressure coefficient ; index 0: Mach number of the undisturbed flow $M_\infty = 0$.) For a slender circular-arc we have (c = chord)

$$-c_{p0\,\max} = \frac{2}{\pi}\frac{c}{\bar{R}}. \qquad (8)$$

Expressing the velocity increases in terms of the pressure coefficient, we find to the first order

$$\frac{V - V_\infty}{V_\infty} = -\frac{c_p}{2}. \qquad (9)$$

Hence from equation (7a) (c_p^* = critical pressure coefficient)

$$\frac{h}{c} = \frac{1}{\pi} \frac{c_p - c_p^*}{c_{p0\,\max}} \quad \ldots \quad (10)$$

Calculating $\bar{\alpha}$ from the average velocity and the average pressure coefficient we find, to a first approximation near the speed of sound

$$\cot \bar{\alpha} = (\bar{M}^2 - 1)^{1/2} = \left[(\gamma + 1)\frac{\bar{V} - V^*}{V^*}\right]^{1/2} = \left[\frac{\gamma + 1}{2}(c_p^* - \bar{c}_p)\right]^{1/2} \quad \ldots \quad (11)$$

Using equation (10) and (11) we get finally for the shift downstream (equation (6))

$$\frac{\Delta x}{c} = \frac{1}{\pi}\left(\frac{\gamma + 1}{2}\right)^{1/2} \frac{(c_p - c_p^*)(c_p^* - \bar{c}_p)^{1/2}}{c_{p0\,\max}} \quad \ldots \quad (12)$$

c_p^* is function of the Mach number M_∞, $c_{p0\,\max.}$ a function of the profile shape only. c_p is the pressure coefficient obtained by high subsonic theory. $\bar{c}_p$ is a mean pressure coefficient, giving a mean Mach angle of the supersonic region. We will take for $\bar{c}_p$ the mean supersonic c_p on the profile.

Assuming an exact subsonic velocity distribution along the profile and the streamlines ending in the stagnation points given by high subsonic theory, we have also the exact area given by the supersonic velocities plotted against the profile length. In our approximation we can take for the super- and subvelocities the pressure coefficient and for the arc length the length along the x-axis. Thus we also get from high subsonic theory the right $\bar{c}_p$. Using equation (12) we get a corrected pressure distribution for the supersonic part on the aerofoil (Fig. 8).

Formula (12) has to fulfil two conditions. Firstly, the area of the curve of supersonic velocities plotted over the x-axis (more exactly over the arc length of the profile) must not be changed by equation (12), because equation (2a) is assumed to be fulfilled by the high subsonic theory used. As the shift downstream, Δx, depends for a given shape and a fixed M_∞ on the velocity only, the distance apart of points with the same c_p remains unchanged by equation (12), thus the area considered is unchanged, as required.

Further, formula (12) has to give the same value of Δx if the thickness ratio and the Mach number of the undisturbed flow are changed according to the law of similarity in transonic flow (R. & M. 2715), otherwise the pressure distribution would not fulfil this law. According to it, the thickness ratio changes proportionally to the cube of the Prandtl factor, β^3, and the velocity differences and also the pressure cofficients change proportionally to β^2. On slender profiles in incompressible flow the pressure coefficient $c_{p0\,\max}$ is proportional to the thickness ratio, hence Δx is the same in similar cases, as required.

There are no doubt several ways of obtaining formulae of the type of equation (12). For example we could take the local Mach angle in equation (6) with a fixed coefficient. All formulae giving Δx as a function of the velocity only fulfil the area condition. Finally it would not be surprising if we were to get better results by changing the coefficient in equation (12), in view of the very rough approximations used.

5. *Application and Comparison with Tests.*—To apply our theory we use the formula of Kármán-Tsien[6], to calculate the compressible c_p distribution from the incompressible c_{p0}

$$c_p = \frac{c_{p0}}{\beta + (1 - \beta)\frac{c_{p0}}{2}} \quad \ldots \quad (13)$$

In spite of our rough approximations, we do not use the slightly simpler Prandtl rule, because we require the subsonic pressures as exact as possible, so as to restrict the inaccuracy as far as possible to the supersonic part. We prefer here the Kármán-Tsien equation to Krahn's equation[7] because Krahn in the derivation of his formula does not satisfy exactly the equation for absence

of vorticity. However there is not much difference between these two corrections of the Prandtl rule and a more precise investigation would be necessary to find the better formula for our purpose.

In this paper we do not calculate the incompressible pressure distribution for the different profiles investigated. Drawing a curve through the test points in pure subsonic flow, we calculate by equation (13) the pressure distribution at the different Mach numbers M_∞ of the undisturbed flow. In this way we get the curves drawn out in Fig. 9, 12, 15 and 16. Then we calculate the shift downstream of the supersonic velocities by equation (12) (line dotted in the figures). There is, of course, a change only above sonic speed (dotted straight line).

As already mentioned the theoretical subsonic velocity just upstream of the supersonic region is always too high. Downstream of the supersonic region the theoretical subsonic velocities are sometimes very good (Fig. 9c, 12b, and 16b) but in most cases too high. In the cases in which they are too small (Fig. 9f, 15e, and 16c) the supersonic region is too large for us to expect good agreement in view of our assumptions.

The agreement of tests and theory at the forward end of the supersonic region is in general very good but at the rear of the supersonic region it is not so good. Here the area formed by the supersonic velocities in general is greater, and that of the subsonic velocities smaller, than calculated. But we can expect a quite good average pressure downstream of the maximum thickness. The supersonic region itself ends quite closely at the point given by the formula of Kármán-Tsien.

In the case of higher supersonic speeds, *i.e.*, large supersonic regions, sometimes (Fig. 12e and 16c) we get at the rear of the supersonic region 3 different values of c_p. This is not surprising in view of the nature of the calculations. To get also in these cases estimates of drag, the pressure distribution at the rear of the supersonic region should be changed, assuming a normal shock-wave and satisfying the area condition.

If we were now to calculate the drag by integrating the pressure on the profile, we should get very poor results, as this method presumes a very exact pressure distribution on the profile nose. Hence we plot the Kármán-Tsien pressure distribution and our supersonic pressure distribution against y (in the figures, against $2y/\tau c$; τ = thickness ratio) and find the drag, by calculating the difference of the area given by the two curves. Figs. 10 and 13 show these pressure distributions against y. While in Fig. 10 the area difference gives half the drag only, because there is the same effect on the upper and lower surfaces, the area difference in Fig. 13 gives the whole drag. In these two figures, the x/c distribution is plotted under one of the graphs. The values with y near the maximum occupy a small part of the $2y/\tau c$ axis. Hence the pressure distribution there has little influence on the drag. This is the reason why immediately beyond the critical speed the drag does not increase much. Not until the supersonic region covers parts of smaller cross-section, does the change in the pressure distribution become important. Then it depends on how much the region of highest suction moves downstream. This seems to be given quite well by formula (12).

Fig. 14 shows experiments of Göthert[8] (dotted lines). The drag coefficient C_D of the profile NACA 0 00 12—1. 1 30 is plotted against the Mach number M_∞ at different lift coefficients C_L. The full lines drawn are curves calculated on the above theory. They are in very good agreement with the tests. As the lift coefficient varies slightly with the Mach number M_∞, all values are corrected to the mean lift coefficient $C_L = 0{\cdot}45$. Because of the neglect of friction the theoretical drags in general would be expected to be smaller than the experimental.

Given the drag coefficient for zero lift against Mach number for a certain thickness ratio τ, the drag coefficient for other thickness ratios and zero lift can easily be calculated, following the law of similarity near sonic speed (R. & M. 2715). The result comparted with Göthert's[9] tests is shown in Fig. 11. The full curve for 12 per cent thickness ratio is the same as the curve for $C_L = 0$ in Fig. 14. The agreement here too is very good. There is a systematic change from too high theoretical values for the thickest profiles to too small theoretical

values for the slenderest profiles. As the law of similarity in this simplest form is valid for very slender aerofoils only, this small disagreement is not surprising. The larger discrepancy on the 6 per cent profile may also be caused by the greater influence of friction.

Fig. 15 and 16 show theoretical and experimental pressure distribution on aerofoils with a position of maximum thickness at 40 per cent and 50 per cent. Drag tests are lacking in these cases. The drag coefficient probably increases here at higher Mach numbers as for the aerofoil of Fig. 9.

Our theory certainly still gives the drag increase at much higher Mach numbers, as the changes in the pressure curves in Fig. 15d ($M_\infty = 0{\cdot}80$ at $\tau = 15$ per cent) and in Fig. 16b ($M_\infty = 0{\cdot}84$) are quite small.

However we have not calculated any other drag curves and we cannot always expect such good results from our very simple theory. But in general we should get by this method a good idea of the drag properties of an aerofoil just beyond its critical speed.

In the case of bodies of revolution equation (2a) gives the same area condition as in the two-dimensional case. The effect of the move downstream of the suction may here be essentially changed. For instance with the whole supersonic region ahead of the maximum thickness, the suction peak moves not only in the direction of smaller surface angle but also of greater body diameter. Thus sometimes the cross-section occupied by the highest suction may be practically unchanged by the move downstream and the effect on the drag may be very small. It may be fairly simple to modify formula (12) for bodies of revolution and to make similar drag investigations for them.

6. *Summary.*—The drag increase beyond the critical Mach number is calculated by modifying the supersonic part of the Kármán-Tsien pressure distribution on a profile. This is possible when the supersonic regions are not too large. The formula giving the modified pressure distribution is derived very roughly. It may give only one of the main effects appearing when supersonic speeds occur in the flow, and may be changed and calculated more exactly later.

For the calculation of the drag increase the formula is adequate and the agreement of theory and experiment in all examples calculated is very good. Within the approximation of the theory the lift coefficient is practically unchanged. Calculations of the centre of pressure are not made.

I wish to express my best thanks to Mr. A. C. S. Pindar and to Mr. E. P. Sutton for correcting the text of this paper and paper concerning the law of similarity in transonic flow (R. & M. 2715).

REFERENCES

No.	*Author*	*Title, etc.*
1	K. Oswatitsch	Der Luftwiderstand als Integral des Entropiestromes. *Nachrichten der Akad. der Wissenschaften in Göttingen Mathem. Phys. Klasse.* 1945, pp. 88–90.
2	G. Guderley	Die Ursache für das Auftreten von Verdichtungsstössen in gemischten Unterschall-Ueberschallströmungen, S.13. M.A.P.–Völkenrode R. & T. 110.
3	K. Oswatitsch and K. Wieghardt ..	Theoretical Investigations on Steady Potential Flows and Boundary Layers at High Speeds. M.A.P. Völkenrode R. & T. 187. German Ref., LGL Report S.13/1d.

REFERENCES—*continued.*

No.	*Author*	*Title, etc.*
4	J. Ackeret, F. Feldmann, and N. Rott ..	Investigations on Compression Shocks and Boundary Layers in Fast Moving Gases. Fig. 12. Institute for Aerodynamics, E.T.H., Zürich, No. 10. 1946. A.R.C. Report 10,044.
5	K. Oswatitsch	A New Law of Similarity for Profiles, Valid in the Transonic Region. R. & M. 2715. June, 1947.
6	Th. von Kármán	Compressibility Effects in Aerodynamics, Equation (62). *J. of Aero. Sci.;* Vol. 8, p. 337, 1941.
7	E. Krahn	A Correction Term for Prandtl's Rule. 1946. M.A.P. Völkenrode R. & T. 21.
8	B. Göthert	The Increase of Drag of Profiles in the Range of High Subsonic Speeds. Fig. 1. M.A.P. Völkenrode R. & T. 36.
9	B. Göthert	High Speed Tests on Symmetrical Profiles of Various Thickness Ratios in the D.V.L. High Speed Wind Tunnel and Comparison with Measurements in Other Wind Tunnels. Fig. 8. F.B. 1506. M.A.P. Völkenrode R. & T. 94.
10	B. Göthert	Druckverteilungs und Impulsverlustschaubilder für die Profile NACA 0 00 06—1, 1 30 bis NACA 0 00 18—1, 1 30 bei hohen Unterschallgeschwindigkeiten. F.B. 1505/1 bis 1505/5. M.A.P. Völkenrode R. & T. 404.
11	B. Göthert and G. Richter	Tests on the Profile NACA 00 15—64 in the High Speed Wind Tunnel of the D.V.L. (2·7 m dia.). Fig. 7. F.B. 1247. M.A.P. Völkenrode R. & T. 414.
12	H. W. Liepmann	Investigations of the Interaction Between Shock Waves and Boundary Layer in Transonic Flow. Fig. 7a, 8a, 9a, 10a, 11a, 12a. *J. of Aero. Sci.*, Vol. 13, p. 623. December, 1946.

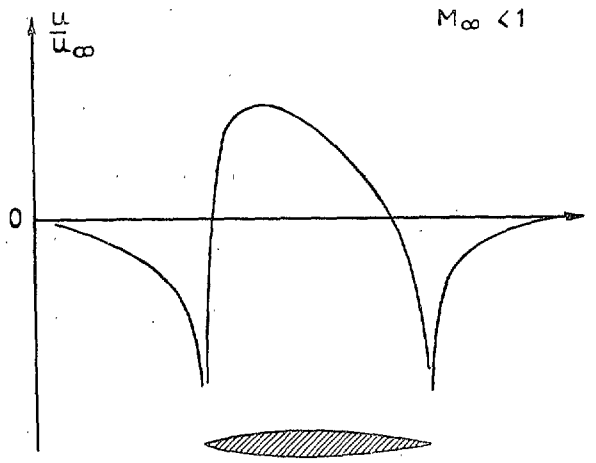

FIG. 1. Velocity distribution on an aerofoil in pure subsonic flow.

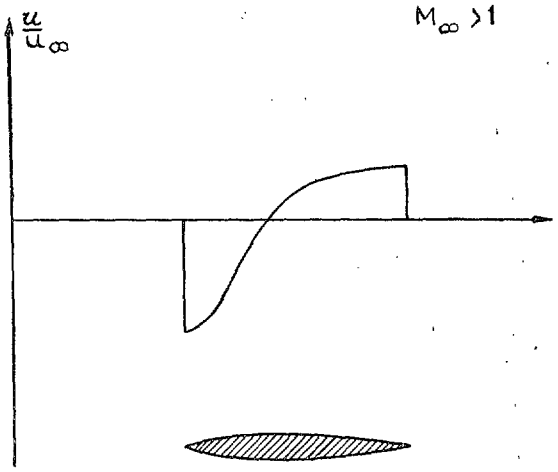

FIG. 2. Velocity distribution on an aerofoil in pure supersonic flow.

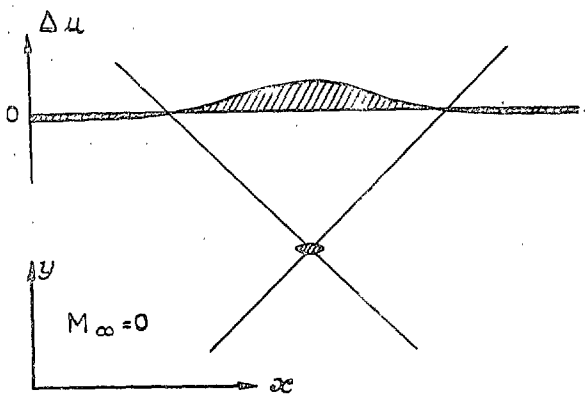

FIG. 3. Velocity disturbance at great distance from a body in two-dimensional incompressible flow.

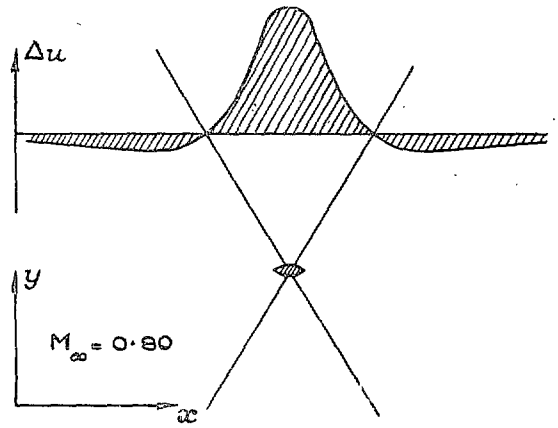

FIG. 4. Velocity disturbance at great distance from a body in two-dimensional flow at Mach number $M_\infty = 0{\cdot}80$.

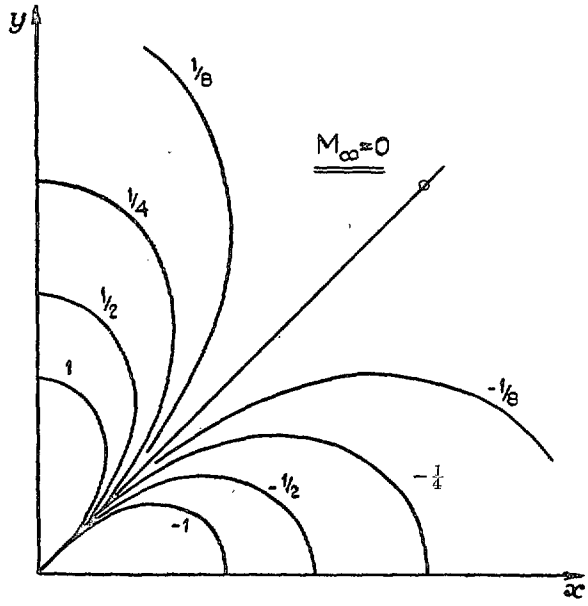

FIG. 3a. Curves of constant influence in two-dimensional incompressible flow.

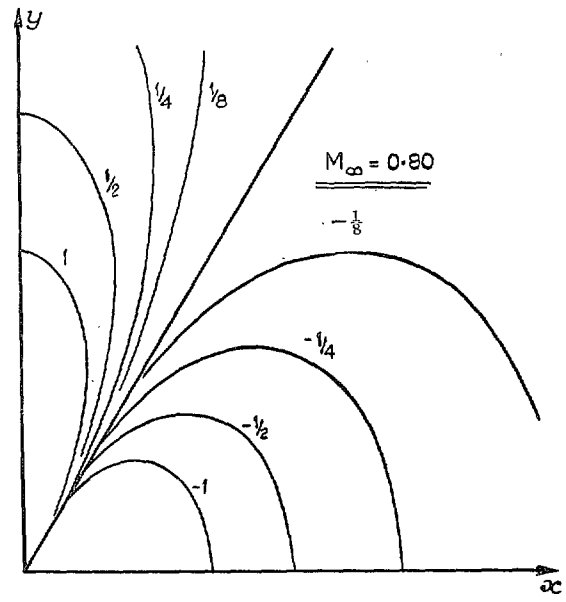

FIG. 4a. Curves of constant influence in two-dimensional flow at Mach number $M_\infty = 0{\cdot}80$.

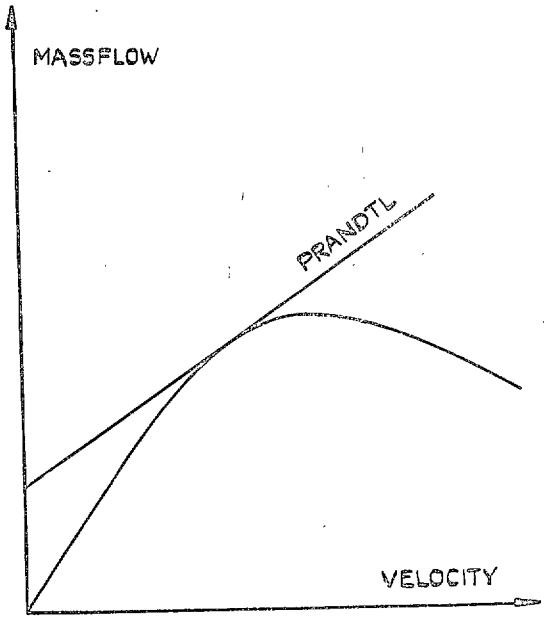

FIG. 5. Mass flow and Prandtl approximation plotted against the velocity.

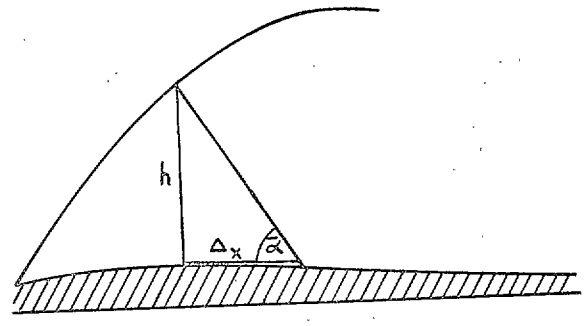

FIG. 7. Effect of a local supersonic region.

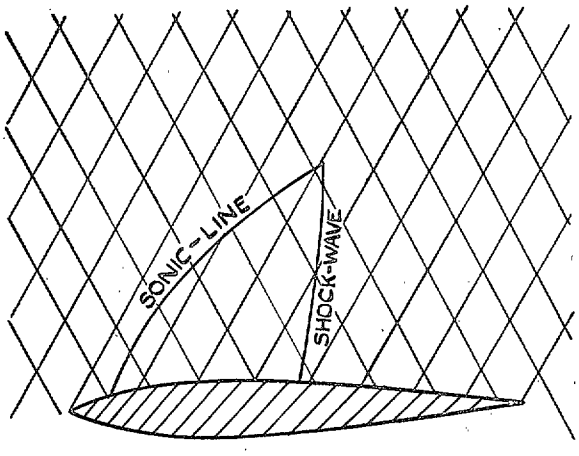

FIG. 6. Supersonic region on an aerofoil and lines of zero influence at Mach number $M_\infty = 0{\cdot}80$.

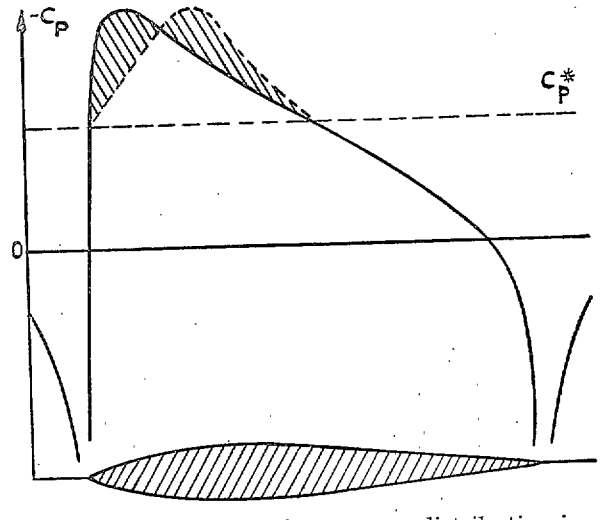

FIG. 8. Change in the pressure distribution in the supersonic region, from consideration of the supersonic properties.

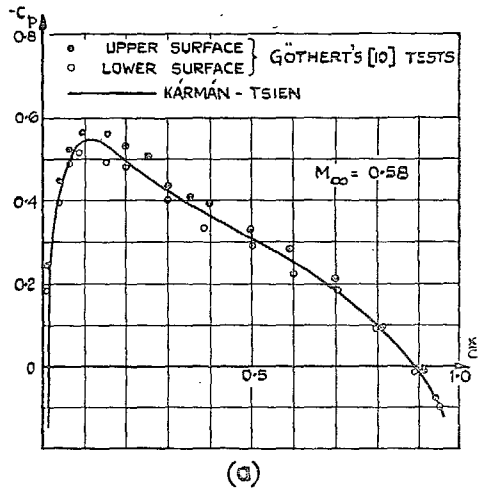

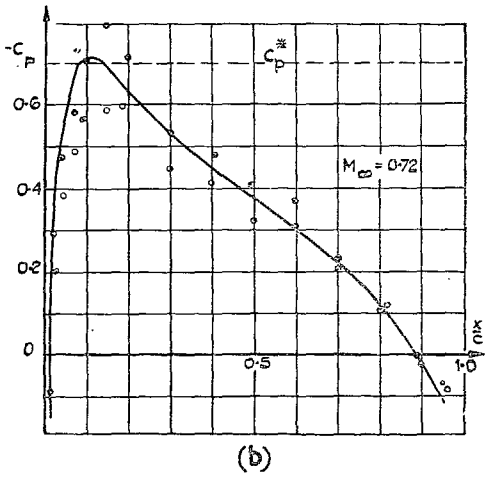

FIGS. 9a and 9b. Pressure distribution on the profile NACA 0 00 12—1. 1 30 at various Mach numbers and zero angle of attack.

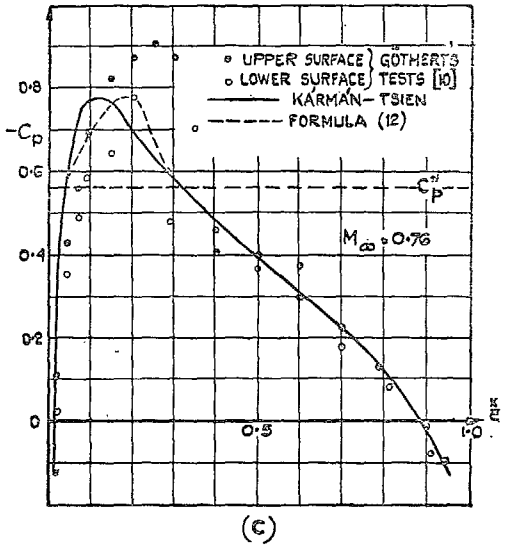

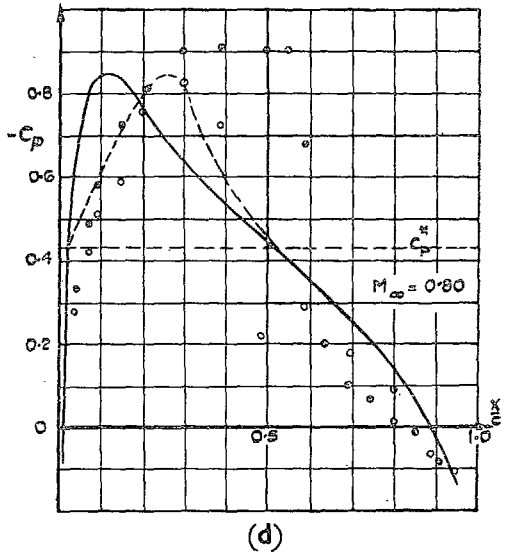

FIGS. 9c and 9d. Pressure distribution on the profile NACA 0 00 12—1. 1 30 at various Mach numbers and zero angle of attack.

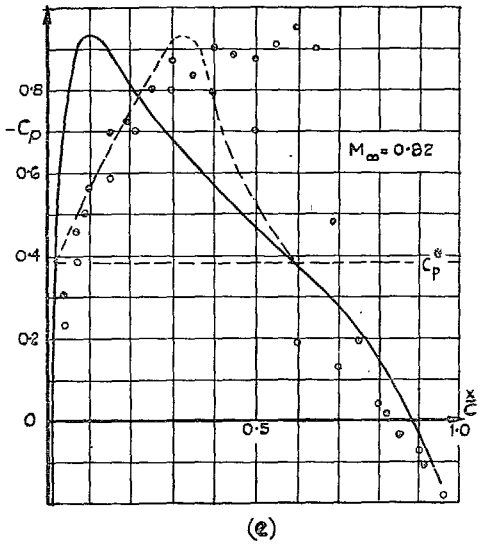

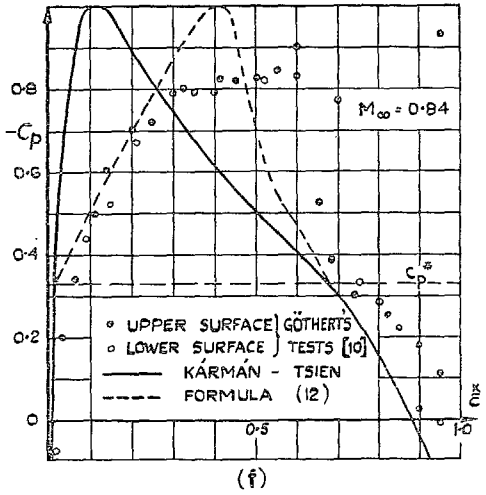

FIGS. 9e and 9f. Pressure distribution on the profile NACA 0 00 12—1. 1 30 at various Mach numbers and zero angle of attack.

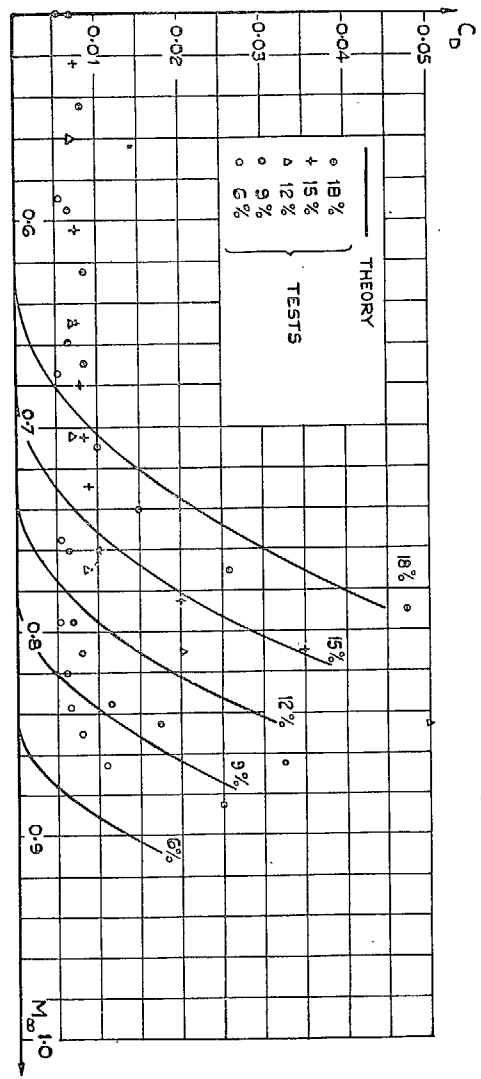

FIG. 11. Drag coefficient C_D of the profile series NACA 0 00 06—1. 1 30 to NACA 0 00 18—1. 1 30 at zero angle of attack plotted against the Mach number M_∞.

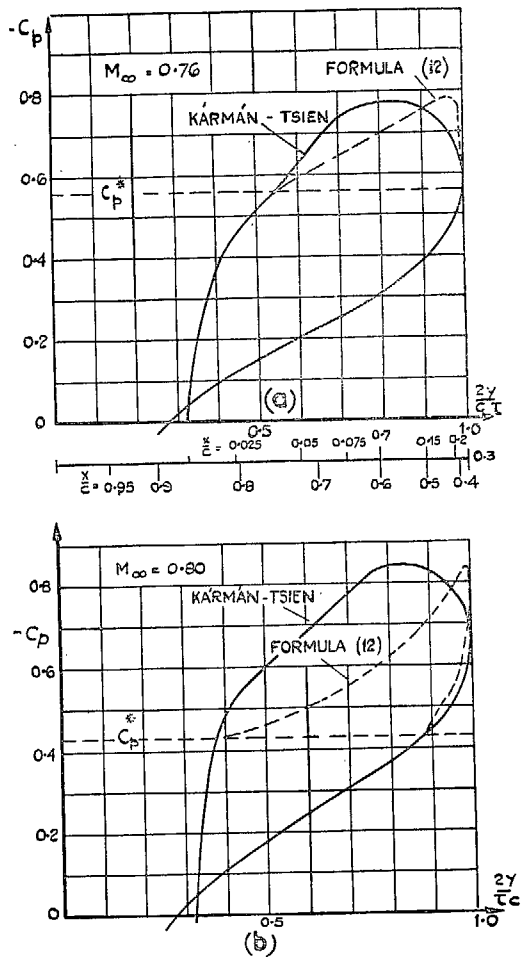

FIGS. 10a and 10b. Pressure distribution of Fig. 9 plotted against y (c chord; t thickness ratio).

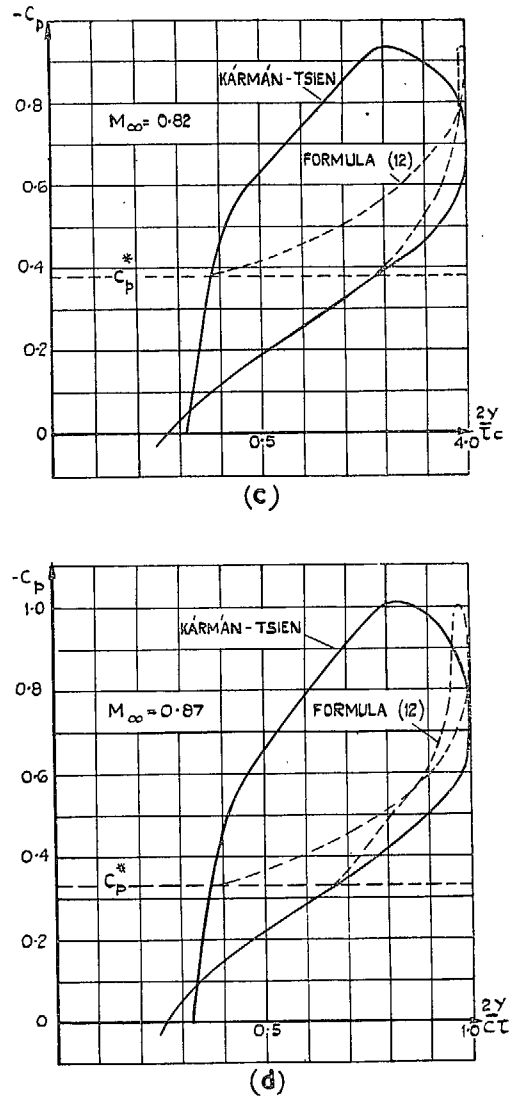

FIGS. 10c and 10d. Pressure distribution of Fig. 9 plotted against y (c chord; t thickness ratio).

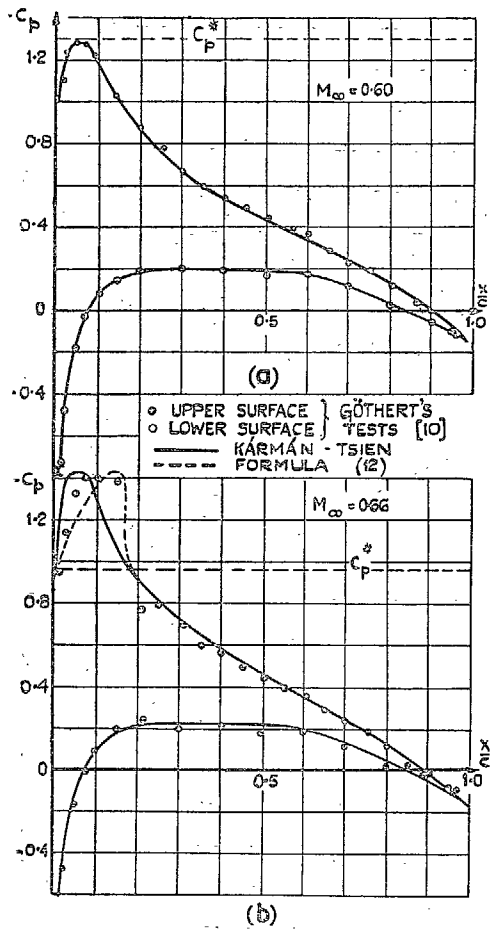

FIGS. 12a and 12b. Pressure distribution on the profile NACA 0 00 12—1. 1 30 at various Mach numbers and 3 deg angle of attack.

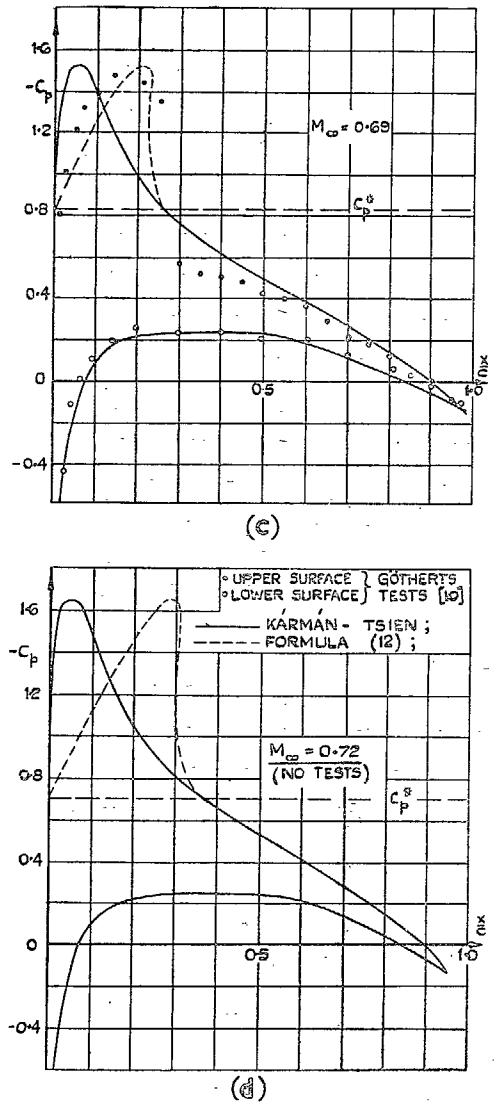

FIGS. 12c and 12d. Pressure distribution on the profile NACA 0 00 12—1. 1 30 at various Mach numbers and 3 deg angle of attack.

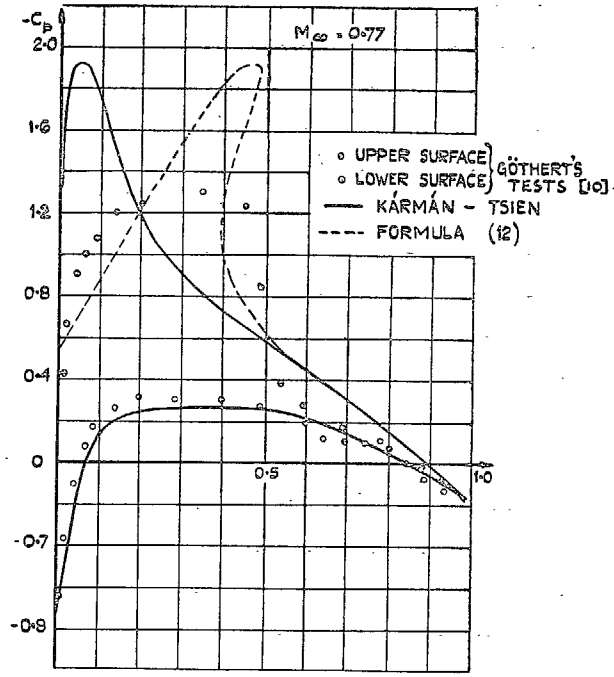

FIG. 12e. Pressure distribution on the profile NACA 0 00 12—1 1. 30 at various Mach numbers and 3 deg angle of attack.

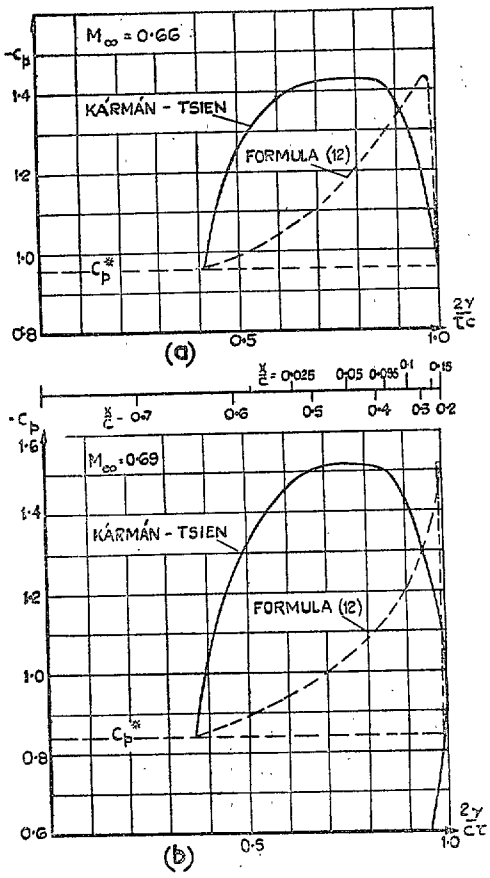

FIG. 13a and 13b. Pressure distribution of Fig. 12 plotted against y (c chord ; t thickness ratio).

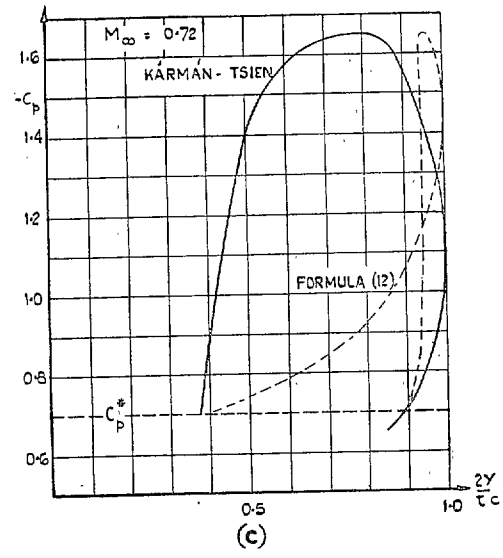

FIGS. 13c. Pressure distribution of Fig. 12 plotted against y (c chord ; t thickness ratio).

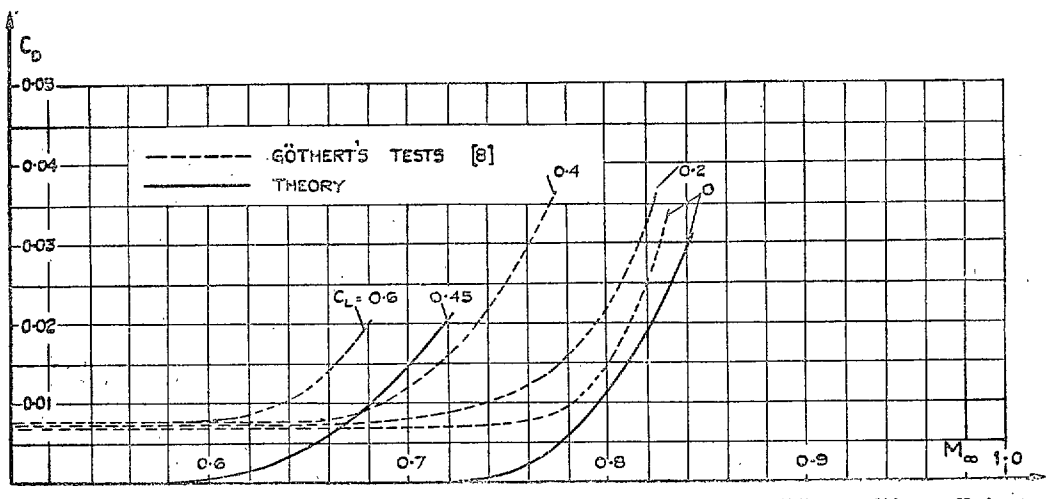

FIG. 14. Drag coefficient C of the profile NACA 0 00 12—1. 1 30 at different lift coefficients C_L.

J4269 Wt.13/806 K7 6/54 D&Co. 34/263

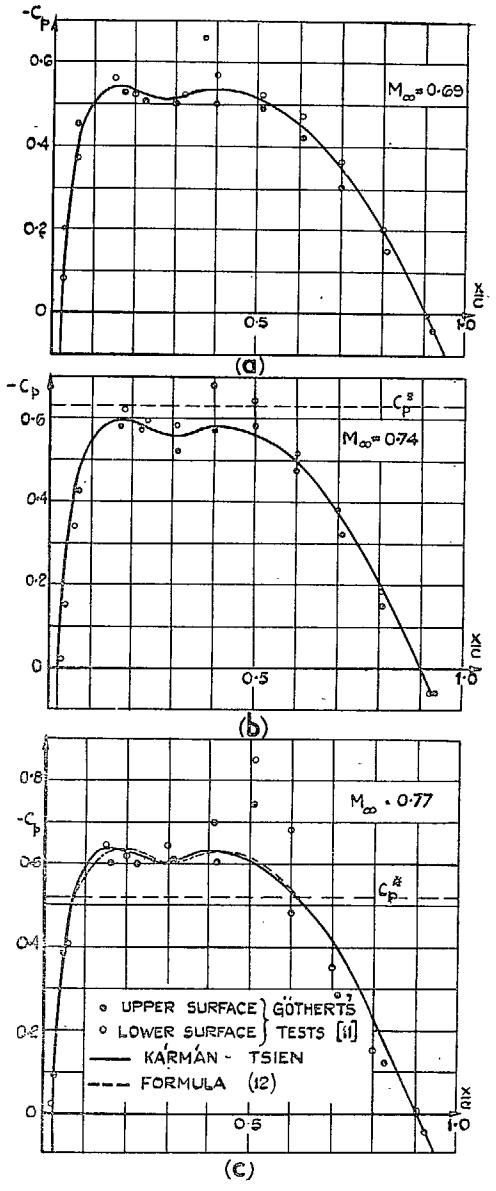

FIGS. 15a, 15b and 15c. Pressure distribution on the aerofoil NACA 00 15—64 at various Mach numbers M_∞ and zero angle of attack.

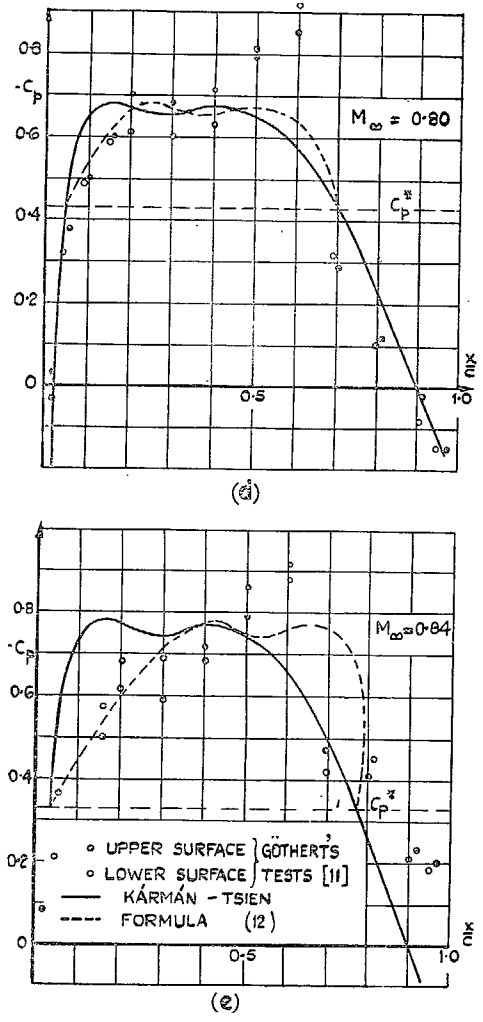

FIGS. 15d and 15e. Pressure distribution on the aerofoil NACA 00 15—64 at various Mach numbers M_∞ and zero angle of attack.

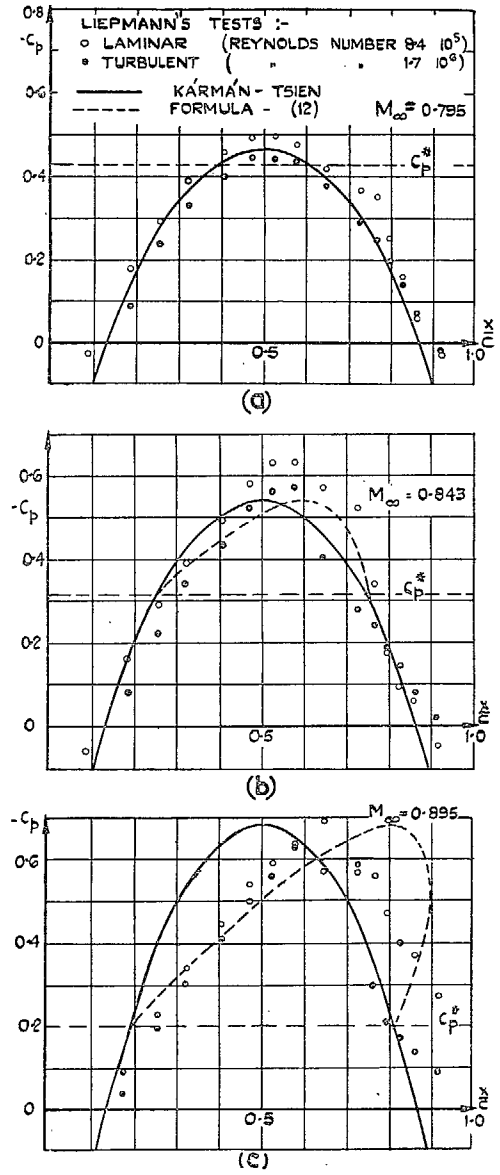

FIGS. 16a, 16b and 16c. Pressure distribution on a circular-arc of 12 per cent thickness.

PRINTED IN GREAT BRITAIN

Publications of the Aeronautical Research Council

ANNUAL TECHNICAL REPORTS OF THE AERONAUTICAL RESEARCH COUNCIL (BOUND VOLUMES)

1936 Vol. I. Aerodynamics General, Performance, Airscrews, Flutter and Spinning. 40*s.* (40*s.* 9*d.*)

Vol. II. Stability and Control, Structures, Seaplanes, Engines, etc. 50*s.* (50*s.* 10*d.*)

1937 Vol. I. Aerodynamics General, Performance, Airscrews, Flutter and Spinning. 40*s.* (40*s.* 10*d.*)

Vol. II. Stability and Control, Structures, Seaplanes, Engines, etc. 60*s.* (61*s.*)

1938 Vol. I. Aerodynamics General, Performance, Airscrews. 50*s.* (51*s.*)

Vol. II. Stability and Control, Flutter, Structures, Seaplanes, Wind Tunnels, Materials. 30*s.* (30*s.* 9*d.*)

1939 Vol. I. Aerodynamics General, Performance, Airscrews, Engines. 50*s.* (50*s.* 11*d.*)

Vol. II. Stability and Control, Flutter and Vibration, Instruments, Structures, Seaplanes, etc. 63*s.* (64*s.* 2*d.*)

1940 Aero and Hydrodynamics, Aerofoils, Airscrews, Engines, Flutter, Icing, Stability and Control, Structures, and a miscellaneous section. 50*s.* (51*s.*)

1941 Aero and Hydrodynamics, Aerofoils, Airscrews, Engines, Flutter, Stability and Control, Structures. 63*s.* (64*s.* 2*d.*)

1942 Vol. I. Aero and Hydrodynamics, Aerofoils, Airscrews, Engines. 75*s.* (76*s.* 3*d.*)

Vol. II. Noise, Parachutes, Stability and Control, Structures, Vibration, Wind Tunnels. 47*s.* 6*d.* (48*s.* 5*d.*)

1943 Vol. I. (*In the press.*)

Vol. II. (*In the press.*)

ANNUAL REPORTS OF THE AERONAUTICAL RESEARCH COUNCIL—

1933–34	1*s.* 6*d.* (1*s.* 8*d.*)	1937	2*s.* (2*s.* 2*d.*)
1934–35	1*s.* 6*d.* (1*s.* 8*d.*)	1938	1*s.* 6*d.* (1*s.* 8*d.*)
April 1, 1935 to Dec. 31, 1936.	4*s.* (4*s.* 4*d.*)	1939–48	3*s.* (3*s.* 2*d.*)

INDEX TO ALL REPORTS AND MEMORANDA PUBLISHED IN THE ANNUAL TECHNICAL REPORTS, AND SEPARATELY—

April, 1950 – – – – R. & M. No. 2600. 2*s.* 6*d.* (2*s.* 7½*d.*)

AUTHOR INDEX TO ALL REPORTS AND MEMORANDA OF THE AERONAUTICAL RESEARCH COUNCIL—

1909–1949 – – – – – R. & M. No. 2570. 15*s.* (15*s.* 3*d.*)

INDEXES TO THE TECHNICAL REPORTS OF THE AERONAUTICAL RESEARCH COUNCIL—

December 1, 1936 — June 30, 1939.	R. & M. No. 1850.	1*s.* 3*d.* (1*s.* 4½*d.*)
July 1, 1939 — June 30, 1945.	R. & M. No. 1950.	1*s.* (1*s.* 1½*d.*)
July 1, 1945 — June 30, 1946.	R. & M. No. 2050.	1*s.* (1*s.* 1½*d.*)
July 1, 1946 — December 31, 1946.	R. & M. No. 2150.	1*s.* 3*d.* (1*s.* 4½*d.*)
January 1, 1947 — June 30, 1947.	R. & M. No. 2250.	1*s.* 3*d.* (1*s.* 4½*d.*)
July, 1951 – – – –	R. & M. No. 2350.	1*s.* 9*d.* (1*s.* 10½*d.*)

Prices in brackets include postage.

Obtainable from

HER MAJESTY'S STATIONERY OFFICE

York House, Kingsway, London W.C.2 ; 423 Oxford Street, London W.1 (Post Orders : P.O. Box No. 569, London S.E.1) ; 13A Castle Street, Edinburgh 2 ; 39 King Street, Manchester 2 ; 2 Edmund Street, Birmingham 3 ; 1 St. Andrew's Crescent, Cardiff ; Tower Lane, Bristol 1 ; 80 Chichester Street, Belfast OR THROUGH ANY BOOKSELLER

S.O. Code No. 23-2716